Journal of Building Engineering 89 (2024) 109303

Contents lists available at ScienceDirect

Journal of Building Engineering

journal homepage: www.elsevier.com/locate/jobe

Seismic performance assessment of a low-rise thin reinforced concrete wall building with unconnected fiber reinforced elastomeric isolators using real-time hybrid simulations

Bryan Castillo, MSc. *, Sharick M. Vides, MSc, Johannio Marulanda, PhD., Albert R. Ortíz, PhD., Peter Thomson, PhD.

School of Civil and Geomatic Engineering, Universidad Del Valle, Santiago de Cali, Colombia

ARTICLE INFO

Keywords:
Real-time hybrid simulation
Base isolator
Thin concrete reinforced wall
Unconnected fiber reinforced elastomeric isolator

ABSTRACT

Thin reinforced concrete wall (TRCW) buildings have become one of the most cost-effective and fastest options for housing construction. However, the performance of the TRCW building under seismic loads has limited energy dissipation capacity and is characterized by brittle failures with dimensions below those limited in international standards, which classifies these walls as ultra-thin. By contrast, unconnected fiber-reinforced elastomeric isolator (U-FREI) devices are a type of seismic isolators with a high deformation capacity, low-cost development, and simplified manufacturing and installation process. To leverage the advantages of both mentioned systems in a combined manner and reduce the structural vulnerability of this type of buildings, this study presents an evaluation of the seismic performance of unconnected fiber-reinforced elastomeric isolator (U-FREI) devices as a base isolation system for low-rise thin reinforced concrete wall (TRCW) buildings using real-time hybrid simulations (RTHS) as an innovative testing technique. RTHS, as a novel physical cybernetic testing technique, allows a dynamic system of interest to be sub-structured into two components: numerical and experimental. The numerical substructure used in this study corresponds to a 24 degrees of freedom (DOF) model that represents the dynamic behavior of a reference low-rise TRCW building. Moreover, the experimental substructure consisted of scaled U-FREI devices that replicated the dynamic response of the base isolation system of the building. To develop an interface between the two substructures, a horizontal transfer system (HTS) was implemented and coupled with a vertical transfer system (VTS). Using RTHS, the performance of the isolated TRCW building was evaluated under four seismic events: El Centro, Kobe, Loma Prieta, and Morgan, at a maximum acceleration of 0.70 g (6.87 $m \bullet s^{-2}$). The implementation of U-FREI devices as base isolation system in a low-rise TRCW building allowed a reduction of the maximum drift by over 54.80 % in comparison with the fixed structure. Finally, the U-FREI devices seismic performance is discussed.

1. Introduction

Structural engineering, which is globally focused on developing technically and economically advantageous buildings to address urban housing demands and rapid construction sector expansion [1], has evidenced the increased implementation of the industrialized

* Corresponding author.
E-mail address: bryan.castillo@correounivalle.edu.co (B. Castillo).

https://doi.org/10.1016/j.jobe.2024.109303
Received 8 November 2023; Received in revised form 6 April 2024; Accepted 9 April 2024
Available online 11 April 2024

system of housing construction (ISHC) in Latin America. ISHC employs thin reinforced concrete walls (TRCW) in buildings, offering efficient construction using reusable metal formwork, enabling fast and replicable monolithic castings. This leads to reduced labor and material requirements [2]. In this region, buildings with ISHC typically have a range of 4–15 levels and use TRCW with thicknesses of 8.0–15.0 cm, dimensions below those limited by international standards, which classifies these walls as ultra-thin. These walls incorporate welded reinforcements in a single layer, whereas additional elements with the same thickness as the wall edge, which are composed of ductile steel, serve as longitudinal reinforcements [3].

Although ISHC is a profitable and effective housing construction alternative in Latin America, studies following earthquakes in Chile (2010), New Zealand (2011), and Turkey (2023) have highlighted the limitations in the seismic performance of the TRCW, which include low ductility, limited energy dissipation capacity, out-of-plane instability, and brittle failure [1,4–6]. Specifically, in Colombia, TRCW buildings have high slenderness coefficients with a single layer of electrowelded reinforcement that meets the minimum requirements specified in Colombian seismic-resistant construction regulations (NSR-10) [7,8]. However, this reinforcement configuration increases susceptibility to out-of-plane instability [9,10]. This condition compromises concrete confinement during high flexural compression demands at the thin ends of the TRCW and propagates construction problems [11]. Additionally, the use of low-ductility reinforcements limits the displacement capacity of TRCW [10].

The ISHC has been implemented in areas of considerable seismic risk, primarily within the Pacific fault zone. In particular, Colombia has geological and seismological conditions that cause 87.0 % of the population to live in these risk areas [7], and ISHC ranks as the first most utilized building system for the construction of residential housing [12]. However, the suitability of ISHC as a primary structural resistance system for building construction in active seismic zones has been questioned due to the inadequate structural performance observed in a wide range of TRCW buildings subjected to seismic loads, even for greater wall thicknesses with a relatively better distribution of ductile reinforcement [4,13].

Structural Engineering has focused on developing techniques to mitigate the seismic vulnerability of systems, such as ISHC, and promoting resilient designs that prioritize occupant safety [14,15]. In order to address these requirements, structural control systems have been widely studied and implemented to improve the dynamic response of civil structures using external devices [17,19], such as passive control systems [18,19], active control systems [16,20], semi-active [18,21], and hybrid control systems [22,23]. Passive control devices have been widely adopted in the construction industry due to their low installation and maintenance costs and lack of energy requirements. Among these, base isolation systems have become reliable and cost-effective alternatives for reducing the seismic vulnerability of buildings [19,24,25]. The aim of these devices is to create a low-rigidity horizontal layer between the structure and its foundation, which concentrates the deformation generated by seismic loads and decreases the energy induced in the structure [26]. This allows for improved behavior in the superstructure to reduce structural damage, repair costs, and the risk of building functionality [27]. Steel-reinforced multilayer elastomeric isolators (SREIs) are the most used isolation devices [28], and their low profitability is due to the complexity of their manufacturing techniques [29]. In Latin America, the expense of importing SREIs hinders widespread implementation [24]. However, fiber-reinforced elastomeric isolators (FREIs) have been proposed as alternatives to SREIs, in which steel-reinforcing plates are replaced with fiber laminates with similar mechanical characteristics [30,31]. FREIs were developed without a mechanical connection to the structure and foundation and are known as unconnected fiber-reinforced elastomeric isolators (U-FREIs). Consequently, U-FREIs facilitate complex manufacturing and installation processes, thereby reducing device weight and cost [24,27,32]. Pauletta et al. [32,33] developed experimental tests to characterize the dynamic behavior of U-FREI devices, and Spizzuoco et al. [34], and Madera et al. [24] in laboratory conditions. Losanno et al. [35] used U-FREI for the base isolation of a symmetrical 2-DOF steel-concrete structure, which was subsequently reproduced by Riascos et al. [36], and Castillo et al. [37], with hybrid control system. In a recent study, Losanno et al. [38] and Calabrese et al. [39], used U-FREI devices as base isolation for the reduction of seismic vulnerability of unreinforced masonry (URM) buildings, which share the same structural system principle (shear wall) as TRCW buildings, demonstrating its potential applicability to the ISHC.

Testing large-scale U-FREI devices under seismic loads requires extensive technical and economic resources. In recent years, an innovative testing methodology known as Real-Time Hybrid Simulation (RTHS) has been used to evaluate the dynamic behavior of complex structural systems or highly nonlinear structures [40–42]. In the RTHS test, the most critical or interesting portion of the system, which generally exhibits nonlinear behavior, was experimentally tested, including inertial effects [43–45] unlike online testing [46]. This testing methodology is ideal for the assessment of highly nonlinear devices, such as base isolation systems, such as those carried out by Lanese et al. [47], Nakata et al. [48], Riascos et al. [49], and Castillo et al. [50], using U-FREI devices, whereas the rest of the isolated TRCW building was assessed analytically with high accuracy using an analytical model. Both components are referred to as experimental and numerical substructures, respectively. These substructures generate a communication interface in real-time through transfer systems to establish a means of interaction between the substructures, thereby creating a communication loop to estimate the dynamic response of the system at each time step [51,52].

The versatility, potential, and acceptable accuracy of RTHS test to concentrate resources on the evaluation of the experimental component of the system results in lower experimental setup costs, increased execution times, and improved performance in the face of the capacity limitations commonly present in large-scale traditional dynamic experimentation [53,54]. In an effort to push the boundaries of research in TRCW buildings and base isolation systems, this study presents an evaluation of the seismic performance of a low-rise TRCW building with scaled U-FREI devices as base isolation using the RTHS technique. These tests were conducted to assess the reduction in the seismic vulnerability of this type of building and validate the use of U-FREI devices for base isolation in the ISHC. Hybrid tests were performed by coupling a unidirectional shake table within the framework of scale model isolator tests at the University of Valle, in Colombia, as a transfer system. The remainder of this paper is organized as follows. Section 2 provides details of the assessed reference structure and a description of the U-FREI devices, their design, and characterization. In Section 3, the dynamic substructuring of the isolated TRCW building with U-FREI devices, the transfer systems employed, the experimental setup, and the seismic excitations are described. A detailed analysis of the seismic performance of the U-FREI devices and the low-rise TRCW building with U-FREI devices as base isolators is presented in Section 4. In this section, the performance of RTHS is evaluated. Finally, Section 5 presents the conclusions of the study.

2. Main structure

2.1. TRCW building

A typical low-rise TRCW building located in Cali-Colombia was chosen as the reference structure. This structure is composed of reinforced concrete thin walls and flat slabs with 8.0 cm and 10.0 cm thickness, respectively, and $f'_c = 24.5$ MPa. The plan dimensions of the building are 13.70 m × 16.50 m with 2.50 m floor height, shown in Fig. 1 a. The distribution of the thin walls is shown in Fig. 1 b, corresponding to an area mean density of 2.0 % and 2.5 % in the X- and Y-directions, respectively. In order to ensure uniform load distribution, a solid slab of 10.0 cm was added, supported on 40.0 cm × 50.0 cm and 40.0 cm × 40.0 cm beams under the walls, which direct the load to 12 U-FREI disposed as shown in Fig. 1 a, which configures the base isolation system of the TRCW building. This isolated structure was modelled in the finite element software ETABS using membrane-shell-type elements for the slabs, shell-thin elements for the thin-walls, and frame elements for the beams, assuming a rigid diaphragm at all levels. The first and second vibration modes in the X and Y directions have frequencies of 0.52 Hz, respectively, which corresponded to the target period of 1.92 s.

2.2. TRCW building isolator system: U-FREI seismic devices

According to FEMA 450 [55] and the methodology proposed by Refs. [24,35] for U-FREI design and structural geometry, 12 full-scale type isolators were dimensioned for the micro zone 1 design spectrum in the city of Santiago de Cali [56]. The rubber height, $H_r = 340\ mm$, was estimated to allow 100 % of the maximum displacement, D_{Max}, without damage to the device. Sixty-two rubber layers and Sixty-one fiber layers were assumed with thicknesses of $t_r = 5.5\ mm$ and $t_f = 1.0\ mm$, respectively, for an isolator total height $H = 400\ mm$.

Rubber height for experimental isolators $H_R^* = 30.0$ mm was taken, according to the form scale factor $F_H = H_r * H_R^{*\,-1} = 11.37$; the relation between diameter and rubber height $D * H_r^{-1} = 2.67$ was maintained for real and reduced scale cases, resulting in a specimen diameter of $D^* = 80.0$ mm. However, there is a loss of stiffness in the scaled U-FREI devices due to shape scaling which was corrected by a stiffness factor $F_R = K_r * K_R^{*\,-1} = 11.52$, these factors are based on the similarity theory. Furthermore, the ratio of the degradation and effective damping values (β_{eff}) were determined as 0.41 and 14.0 %, respectively. Based on these data, two reduce-scale U-FREI specimens (P1 and P2), shown in Fig. 2 a, were fabricated, consisting of 15 rubber layers of 2.00 mm thick and reinforced by 14 polyester fiber layers of 1.00 mm thick as shown in Fig. 2 b. The specimens were simultaneously subjected to shear and compression loads by applying a sinusoidal lateral displacement protocol with approximate deformation levels, γ, of 38 %, 56 %, 88 %, 117 %, 146 %, and 175 %. Simultaneously, a constant vertical load of 19.0 kN was applied. The hysteretic behavior of a pair of isolators U-FREI (P1 and P2), which were designed and built with the same parameters and materials, is shown in Fig. 3 a, where a high inherent nonlinearity of the elastomeric materials was observed. Although, the differences between the same specimens are due to the manufacturing processes and intrinsic variability of the materials from which they are composed, the experimental shear rubber modulus for both is close to the design deformation performance levels of the U-FREI devices, decreasing the impacts of their variability. In all cases, there was a reduction in stiffness compared with the first cycle for each level of deformation owing to the Mullins effect [24,31]. The effective stiffness K_h and damping coefficient β_i were calculated using Equations (1) and (2), respectively.

$$K_{h,i} = \frac{F_{max,i} - F_{min,i}}{D_{max,i} - D_{min,i}} \tag{1}$$

$$\beta_i = \frac{E_{d,i}}{2 \bullet \pi \bullet K_{h,i} \bullet D_{max,i}^2} \tag{2}$$

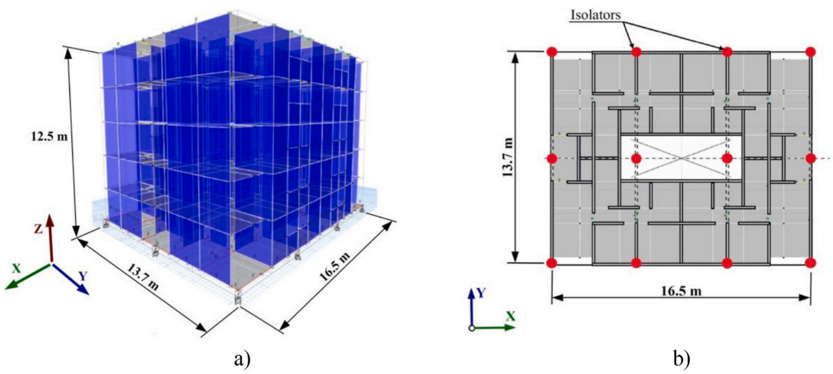

Fig. 1. Reference structure. a) Isometric view of model in software ETABS, and b) plan location of U-FREIs devices.

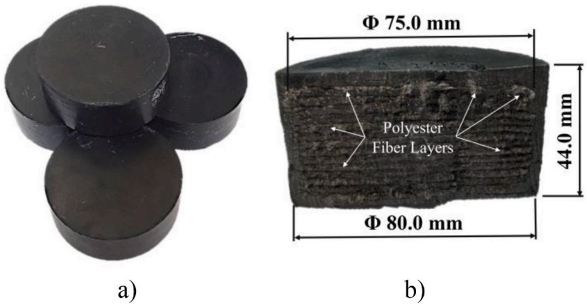

Fig. 2. U-FREIs Device. a) U-FREIs experimental specimens, and b) Isolator cross-section diagram.

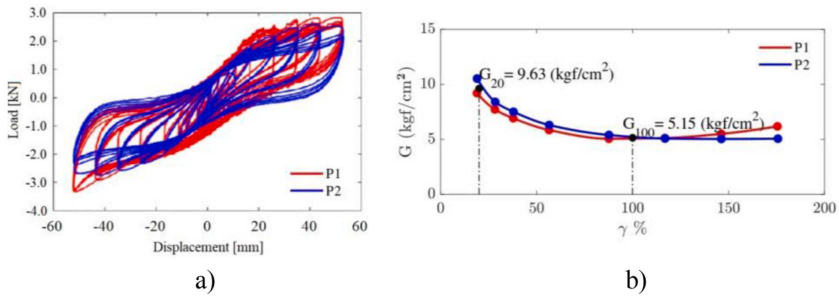

Fig. 3. Dynamic behavior of U-FREI devices. a) Hysteretic behavior of experimental U-FREI specimens, and b) Experimental shear rubber modulus.

Where $F_{\max,i}$, $F_{\min,i}$, $D_{\max,i}$, and $D_{\min,i}$ correspond to the maximum and minimum values of load and displacement in each hysteresis cycle. These parameters are listed in Table 1, in which there is correspondence between the specimens for deformation levels close to 100 %, which is the design level of the U-FREI devices in this study, with lateral effective stiffness $K_h \approx 73.30\ kN \bullet m^{-1}$ and damping coefficient $\beta_i \approx 12.46\%$. In addition, Fig. 3 b shows the behavior of the shear modulus G for different deformation levels, being the most important at 20.0 % ($G_{20} \approx 10.0\ kgf \bullet cm^{-2}$) and 100.0 % ($G_{100}, \approx 5.0\ kgf \bullet cm^{-2}$), where the design process of the specimens is feedback [24,49].

3. Real-time hybrid simulation (RTHS)

3.1. Numerical substructure (NS)

The Y-axis behavior of the low-rise TRCW building, shown in Fig. 1, without the dynamic properties of the proposed base isolation system, was analyzed using an analytical multiplex-Degrees of freedom model, which constituted the numerical substructure (NS). This is based on the premise that U-FREI devices can maintain the elastic range of the TRCW structure. To adjust the model, elements simulating generic isolating devices were included to obtain accuracy, the roll-out effect that developed by these devices, and the vertical stiffness (K_v) that allows deformation in that direction of movement [44]. An analytic model of the full-scale TRCW building with an isolated base composed of 12 nodes and 28 elements was developed using the Finite Element Method (FEM), and the dynamic responses of this model were adjusted to the response obtained in the model developed using ETABS software, according to *Section 2.1*, with a sinusoidal excitation in the base with constant amplitude and a frequency range of 0.10–20.0 Hz. Initially, the analytic model was proposed with 36 Degrees of freedom (DOF), considering frame-type elements with 3 DOF per node (Fig. 4 *a*). Then, the static condensation method was used, and the model was simplified to 24 DOF, considering only translational movements (Fig. 4 *b*) and the distribution of masses shown in Fig. 4 *c*. The dynamic behavior of the structure is governed by Eq. (3), where M_r, C_r and K_r are the mass,

Table 1
U-FREIs Mechanical properties.

Def. (%)	K_{eff} (kN/m)				β_{eff} (%)			
	Numerical	P_1	P_2	*Δ Exp. (%)*	Numerical	P_1	P_2	*Δ Exp. (%)*
175.50	64.23	55.73	41.24	26.00	11.22	15.54	20.77	33.66
146.40	67.28	60.48	54. 01	10.70	12.07	13.23	14.66	10.81
116.90	71.86	68.86	66.20	3.86	12.73	12.46	12.77	2.49
87.70	79.46	77.48	80.64	4.08	12.51	12.68	11.94	5.84
56.60	94.68	97.02	103.20	6.37	8.94	12.30	11.27	8.37
38.00	107.17	115.61	124.17	7.40	4.49	12.04	10.78	10.47

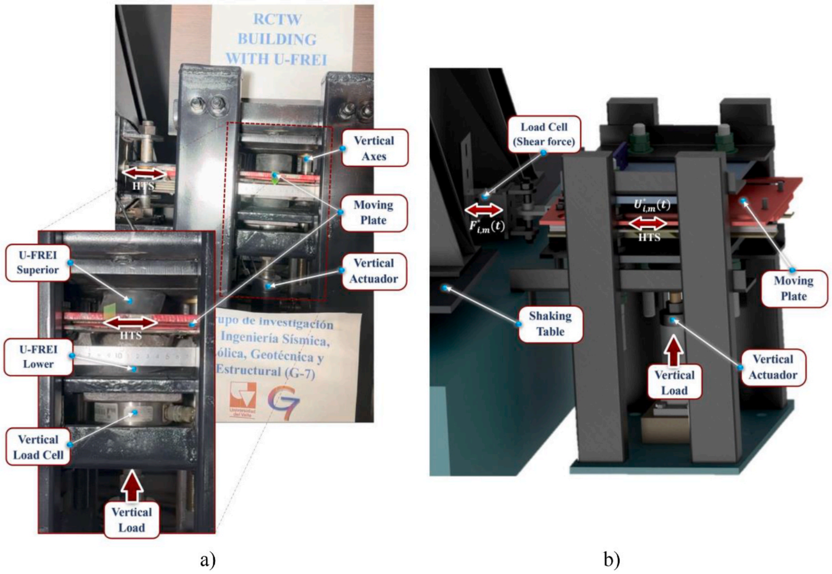

Fig. 5. Small-Scale Framework. a) Experimental small-scale framework for testing small-scale isolators, and b) scheme of operation of the small-scale framework.

In order to apply the load acting on the U-FREI devices, a vertical transfer system (VTS) consisting of a hydraulic power unit (HPU) and vertical actuator was connected to a load cell to measure the compression force. However, it is important to note that U-FREIs exhibit a roll-out effect that directly affects their deformation [32,36,49]. This phenomenon consists of a roll-out deformation assumed by the isolator device subjected to a compression load and a relative displacement between its supports, producing a progressive detachment of the zone that was initially in full contact with the supports [31,33]. Owing to this dynamic behavior of vertical movement, a control system for the actuator was implemented to maintain a constant load despite the variable deformation of the specimen during different deformation states in the simulation, as described in Ref. [49]. However, in this study, a servo valve, *EATON KBS-10,* was used to control an actuator with asymmetric behavior by implementing a proportional integral (PI) controller with constants k_p and k_i, which provides high accuracy in the behavior of the VTS. The controller loop provided feedback from the normal restoring force N_m measured from the specimens.

3.4. Experimental setup

The numerical and experimental substructures and transfer systems were interconnected according to the scheme shown in Fig. 6 to develop of the RTHS. The numerical substructure is subjected to an input signal corresponding to the base acceleration $\ddot{a}_g$ (seismic event); the numerical substructure responds to this excitation according to its dynamic properties and the isolated base shift response $u_{i,d}$ is taken and scaled with the shape factor ($F_H{}^{-1}$). The scaled signal $u^*_{i,d}$ was then sent to the HTS, which was responsible for replicating $u^*_{i,m}$ and transmitting it to the experimental U-FREI device system. Simultaneously, the VTS applied a vertical load to frame N_m, causing the compression deformation of the tested specimens. The opposing force exerted by the two isolators F^*_m is measured by the load cell, scaled in shape and stiffness with F_H and F_R according to *Section 2.2*, and later multiplied by the number of isolators N_{iso} of the entire system to obtain the total feedback force F_{Feed} of the numerical substructure and close the loop. This process was programmed in the Simulink software and executed with a SpeedGoat processor using a host computer with the Xpc protocol of MATLAB and a sampling frequency of 1024 Hz. SpeedGoat has a high processing capacity to guarantee real-time evaluation of the hybrid simulation.

3.5. Input signal: seismic excitation

The seismic performance of U-FREIs devices as base isolation systems for mitigating the structural vulnerability of TRCW buildings

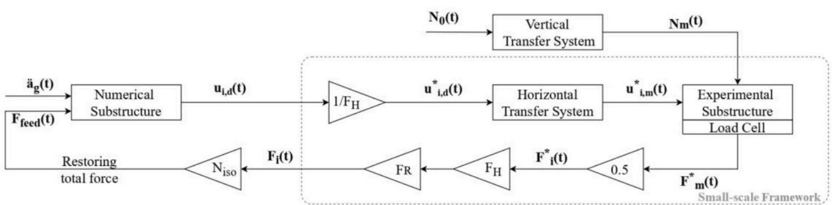

Fig. 6. Real-Time Hybrid Simulation (RTHS) scheme.

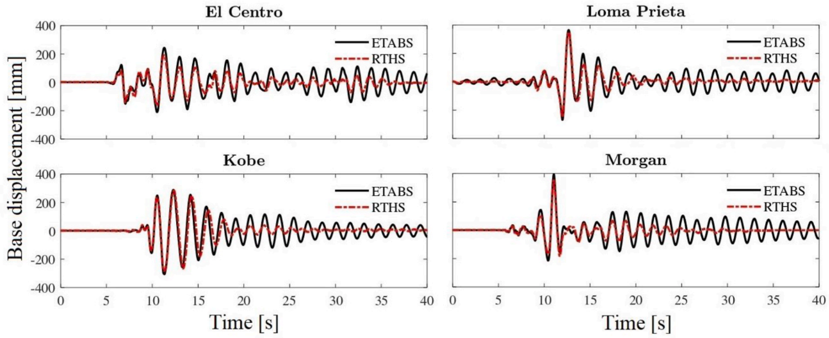

Fig. 8. Base displacement in the time domain for the analyzed seismic event.

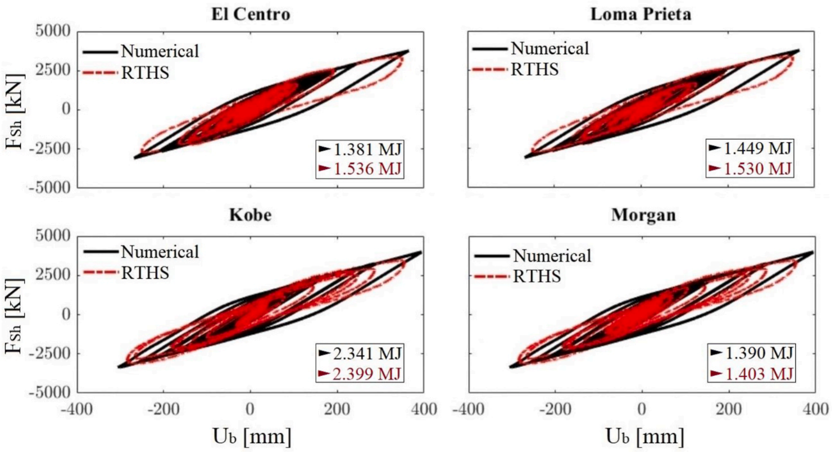

Fig. 9. U-FREI devices Hysteresis cycles for the analyzed seismic event.

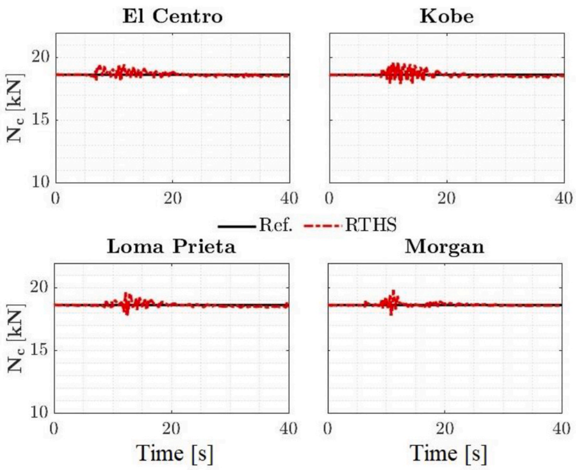

Fig. 10. Vertical load performance during RTHS for the analyzed seismic event.

structure, the electronic noise present in the experimental signals of the ES, and the dynamics of the actuators that are part of the transfer systems [41,54]. Therefore, some indices have been proposed to evaluate the accuracy of the RTHS, considering the possible discrepancies between the reference and experimental signals. Several of these evaluation measures focus on the local response during an HS by considering the physical component and its boundary with the numerical component. The evaluation of local performance was based on the synchronization of the boundary conditions between the numerical response ($u^*_{i,d}$) sent to the actuator and the

Table 2
Reduction of relative displacements and maximum drifts per floor.

CASE		Relative displacement [mm]					Drift [%]				
		Floor 1	Floor 2	Floor 3	Floor 4	Floor 5	Floor 1	Floor 2	Floor 3	Floor 4	Floor 5
EL CENTRO	Without BI	3.24	9.65	17.69	26.28	34.62	0.13	0.26	0.32	0.34	0.33
	With U-FREI	1.86	4.17	6.57	8.98	11.33	0.07	0.09	0.10	0.10	0.09
	Reduction	**42.6 %**	**56.8 %**	**62.9 %**	**65.8 %**	**67.3 %**	**42.6 %**	**64.0 %**	**70.1 %**	**71.9 %**	**71.9 %**
KOBE	Without BI	4.46	13.26	24.27	35.98	47.35	0.18	0.35	0.44	0.47	0.46
	With U-FREI	1.99	4.47	7.05	9.65	12.18	0.08	0.10	0.10	0.10	0.10
	Reduction	**55.5 %**	**66.3 %**	**70.9 %**	**73.2 %**	**74.3 %**	**55.5 %**	**71.8 %**	**76.5 %**	**77.8 %**	**77.7 %**
LOMA	Without BI	2.88	8.36	15.02	21.93	28.58	0.12	0.22	0.27	0.28	0.27
	With U-FREI	2.37	5.32	8.39	11.48	14.48	0.10	0.12	0.12	0.12	0.12
	Reduction	**17.8 %**	**36.4 %**	**44.1 %**	**47.7 %**	**49.3 %**	**17.8 %**	**46.2 %**	**53.8 %**	**55.4 %**	**54.8 %**
MORGAN	Without BI	6.66	19.87	36.50	54.26	71.53	0.27	0.53	0.67	0.71	0.69
	With U-FREI	2.28	5.10	8.05	11.00	13.87	0.09	0.11	0.12	0.12	0.12
	Reduction	**65.8 %**	**74.3 %**	**78.0 %**	**79.7 %**	**80.6 %**	**65.8 %**	**78.6 %**	**82.3 %**	**83.4 %**	**83.4 %**

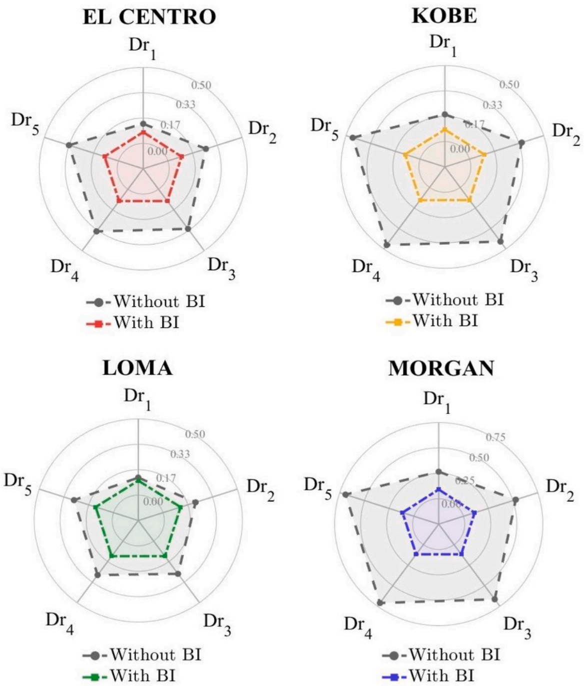

Fig. 11. Comparison maximum drifts of the TRCW building with and without Base Isolator using U-FREI devices.

displacement achieved in the physical component ($u^*_{i,m}$). The normalized root mean square error in the experiment (NRMSE) can be used according to Eq. (7) to obtain a single value that represents the difference between the actuator signals in the time domain. Similarly, for comparison in the frequency domain, Equations (8)–(12) are considered, corresponding to the frequency evaluation index (FEI), which compares the fast Fourier transform (FFT) of the desired signal $u^*_{i,d}$ with that of the measured signal $u^*_{i,m}$ at the actuator, the frequency with the largest share during the RTHS f^{eq}, the generalized amplitude A_0, and the delay δ [61].

$$NRMS_{error} = \sqrt{\frac{\sum_{j-1}^{N}\left[u^*_{i,d}(j) - u^*_{i,m}(j)\right]^2}{\sum_{j-1}^{N}\left[u^*_{i,d}(j)\right]^2}} \tag{7}$$

$$FEI = \sum_{j=1}^{N} \left(\frac{u^*_{i,m}(j)}{u^*_{i,d}(j)} \bullet \frac{\left\| u^*_{i,d}(j) \right\|^{l}}{\sum_{j=1}^{P} \left\| u^*_{i,d}(j) \right\|^{l}} \right) \tag{8}$$

$$f^{eq} = \frac{\sum_{j-1}^{N} \left(\left\| u^*_{i,d}(j) \right\|^{l} \bullet f_i \right)}{\sum_{j-1}^{N} \left\| u^*_{i,d}(j) \right\|^{l}} \tag{9}$$

$$A_0 = \| FEI \| \tag{10}$$

$$\varnothing = arctan \left[\frac{Im(FEI)}{Re(FEI)} \right] \tag{11}$$

$$\delta = -\frac{\varnothing}{2 \bullet \pi \bullet f^{eq}} \tag{12}$$

Additionally, the global indices considered the interaction between the numerical and experimental substructures, and they were evaluated in the time domain, quantifying the largest difference between the calculated and measured displacements using e_{DM} and e_{MD}, as shown in Eqs. (13) and (14) [61].

$$e_{DM} = \frac{\left| \left| u^*_{i,d} \right|^{max} - \left| u^*_{i,m} \right|^{max} \right|}{\left| u^*_{i,m} \right|^{max}} \tag{13}$$

$$e_{MD} = \frac{\left| u^*_{i,d} - u^*_{i,m} \right|^{max}}{\left| u^*_{i,m} \right|^{max}} \tag{14}$$

All indexes were obtained for the four RTHS and are presented in Table 3. All cases presented a high level of horizontal tracking, with a generalized amplitude A_0 close to 1.0, and global errors lower than 4.0 %, which allowed us to conclude that ST as HTS has high performance and allows performing RTHS with a high level of accuracy, which demonstrates its optimal performance during the RTHS. The accuracy and performance of the HTS during the RTHS are shown graphically in Fig. 12 for all the seismic events evaluated, where the red line corresponds to the measured signal and the black line is the reference signal.

5. Conclusion

In this study, a seismic performance assessment of scaled U-FREI devices as system base isolation of a low-rise TRCW building was performed using the RTHS methodology for four seismic events: El Centro, Kobe, Loma Prieta, and Morgan, scaled to an acceleration of 0.70 g (6.87 $m \bullet s^{-2}$). The main conclusions are as follows:

(1) In all seismic events evaluated was observed an increase in the effective damping coefficient of scaled U-FREI experimental devices used as base isolation system (EDC≈12.0 %) for smaller deformations (less 70.0 %) compared with its analytical estimation using a bilinear hysteretic model implemented in ETABS (EDC≈4.0 %). Furthermore, the form scale and stiffness factors used for the scaled U-FREI devices similarity law allow for large-scale hysteretic behavior equivalent to that developed analytically by the bilinear hysteretic model, with an increase in the energy dissipation capacity of the experimental prototypes of 10.09 %, 2.42 %, 5.29 %, and 0.93 % for the El Centro, Kobe, Loma Prieta, and Morgan earthquakes, respectively, compared to the analytical model. This difference is due to the nonlinear hysteretic behavior present in the U-FREI devices, which is limited in the bilinear hysteresis analytical model. In addition, the vertical load variations on the base isolator system of the low-rise TRCW building were less than 7.0 % using the analytical model described in <i>Section 3.1,</i> and the ETABS model, which allowed for a constant vertical load on scaled U-FREI devices without alterations in their hysteretic behavior during RTHS. However, the authors recommend considering this vertical load in HTS for isolated TRCW buildings over 8.0 levels, where the vertical load has a greater influence on the hysteretic behavior of U-FREI devices during RTHS.

Table 3
RTHS evaluation indexes: lateral transfer system.

Seismic	$NRMS_{error}$ (%)	FEI	f_{eq} [Hz]	A_0	e_{DM} (%)	e_{MD} (%)	δ (ms)
El Centro	3.110	0.995–0.041i	1.234	0.996	0.123	3.596	5.200
Kobe	2.570	0.997–0.033i	1.268	0.997	0.092	2.966	4.150
Loma Prieta	2.840	1.002–0.032i	1.273	1.002	0.021	2.836	4.234
Morgan	3.320	1.003–0.053i	1.158	1.004	0.124	3.080	7.256

[46] K. Takanashi, M. Nakashima, Japanese activities on on-line testing, J. Eng. Mech. 113 (7) (1987) 1014–1032, https://doi.org/10.1061/(asce)0733-9399(1987)113:7(1014).
[47] I. Lanese, A. Pavese, F. Dacarro, Development of software and hardware architecture for real-time dynamic hybrid testing and application to a base isolated structure, J. Earthq. Eng. 16 (SUPPL. 1) (2012) 65–82, https://doi.org/10.1080/13632469.2012.675833.
[48] N. Nakata, R. Erb, M. Stehman, Mixed force and displacement control for testing base-isolated bearings in real-time hybrid simulation, J. Earthq. Eng. 23 (6) (2019) 1055–1071, https://doi.org/10.1080/13632469.2017.1342296.
[49] C. Riascos, S. Klopov, D. Losanno, J. Marulanda, P. Thomson, Real-time hybrid simulations including rocking effects: the case of a frame-structure with unbounded elastomeric isolators, Struct. Control Health Monit. 29 (9) (Sep. 2022) e2984, https://doi.org/10.1002/stc.2984.
[50] B. Castillo, D.F. Ceron, S.M. Vides, J. Marulanda, P. Thomson, Comprehensive Assessment of the Seismic Performance of an Innovative Hybrid Semiactive and Passive State Control System for a Low-Degree-Of-Freedom Structure Using Real-Time Hybrid Simulation, vol. 2024, 2024.
[51] J. Sun, J. Xiao, Z. Li, X. Feng, Experimental study on the thermal performance of a 3D printed concrete prototype building, Energy Build. 241 (2021) 110965, https://doi.org/10.1016/j.enbuild.2021.110965.
[52] G. Ou, S.J. Dyke, A. Prakash, Real time hybrid simulation with online model updating: an analysis of accuracy, Mech. Syst. Signal Process. 84 (2017) 223–240, https://doi.org/10.1016/j.ymssp.2016.06.015.
[53] A.H. Schellenberg, T.C. Becker, S.A. Mahin, Hybrid shake table testing method: theory, implementation and application to midlevel isolation, Struct. Control Health Monit. 24 (5) (2017) e1915.
[54] H. Li, A. Maghareh, H. Montoya, J.W. Condori Uribe, S.J. Dyke, Z. Xu, Sliding mode control design for the benchmark problem in real-time hybrid simulation, Mech. Syst. Signal Process. 151 (2021) 107364, https://doi.org/10.1016/j.ymssp.2020.107364.
[55] BSSC, Recommended Provisions for Seismic Regulations for New Buildings and Other Structures (FEMA 450), FEMA, Washington, DC, USA, 2003.
[56] G. del M. A. Instituto Colombiano de Geología y Minería (INGEOMINAS) and Departamento Administrativo de (DAGMA), Informe 5.2 respuesta sismica, Microzonificación Sísmica Santiago de Cali 1 (1) (2005).
[57] C.P. Katsaras, T.B. Panagiotakos, B. Kolias, Restoring capability of bilinear hysteretic seismic isolation systems, Earthq. Eng. Struct. Dynam. 37 (4) (2008) 557–575.
[58] C. Arteta, C. Blandon, R. Bonett, J. Carrillo, Estudio del Comportamiento Sísmico de Edificios de Muros delgados de concreto reforzado, CEER Report 002, no. 002, 2018, pp. 1–100.
[59] H. Gonzales, F. López-Almansa, Seismic performance of buildings with thin RC bearing walls, Eng. Struct. 34 (2012) 244–258, https://doi.org/10.1016/j.engstruct.2011.10.007.
[60] A. Rosso, J.P. Almeida, K. Beyer, Stability of thin reinforced concrete walls under cyclic loads: state-of-the-art and new experimental findings, Bull. Earthq. Eng. 14 (2) (2016) 455–484, https://doi.org/10.1007/s10518-015-9827-x.
[61] A. Christenson, et al., Hybrid Simulation: A Discussion of Current Assessment Measures, 2014.